Effect of pore fluid quality on the behaviour of a kaolin–bentonite mixture during drying and wetting cycles

A. R. Estabragh

Associate Professor, Faculty of Soil and Water Engineering, University of Tehran, PO BOX 4411, Karaj 31587–77871, Iran

ORCID: 0000-0003-4545-2310

Tel: +98 261 2241119

Fax: +98 261 2226181

Email: Raeesi@ut.ac.ir

A. Soltani

PhD Student, School of Civil, Environmental and Mining Engineering, The University of Adelaide, SA 5005, Australia

ORCID: 0000-0002-0483-7487

Tel: +61 8 83132830

Fax: +61 8 83134359

Email: Amin.Soltani@adelaide.edu.au

A. A. Javadi

Professor, Computational Geomechanics Group, Department of Engineering, University of Exeter, Devon EX4 4QF, UK

Tel: +44 1392 723640

Fax: +44 1392 21796

Effect of pore fluid quality on the behaviour of a kaolin–bentonite mixture during drying and wetting cycles

Abstract

The behaviour of a kaolin–bentonite mixture with different pore water quality, i.e. distilled water, NaCl and $CaCl_2$ solutions, was investigated through a number of cyclic drying and wetting tests. Experimental tests were performed on compacted samples of the expansive soil (mixture of 80% kaolin and 20% bentonite) in a modified oedometer with different pore water quality under a surcharge pressure of 10 kPa. The vertical and radial deformations of the samples were determined during different stages of drying and wetting. In addition, the soil–water characteristic curve was established by the filter paper technique for samples with different pore water quality. The results indicate that the shrinking–swelling deformation was nearly the same when the equilibrium condition was attained. Furthermore, the paths of drying and wetting converged to an *S*–shaped curve at equilibrium condition. This curve consists of one linear and two curvilinear portions, and the majority of the deformation occurred in the linear section. The hysteresis phenomenon was also studied through the void ratio and suction, and the results indicated that the hysteresis is gradually disappeared with increasing the number of drying and wetting cycles.

Keywords: Expansive soil; Drying and wetting cycles; Pore water quality; Suction; Soil–water characteristic curve; Void ratio; Hysteresis.

1. Introduction

Expansive soils, also known as shrink–swell or swelling soils, are a group of problematic soils the volume of which is changed due to variations in water content. Their volume is expanded by increasing water content and is shrunk when exposed to drying. Such soils rise or fall periodically when exposed to seasonal water content change, which causes severe damage to highways, structures and low-rise buildings. The annual cost of damage to structures built on expansive soils is estimated about £150 million in the UK, $1000 million in the United States and billions of dollars worldwide (Gourley et al. 1994). The Association of British Insurers has estimated that the average cost of shrink–swell-related subsidence to the insurance industry stands at over £400 million per year (Driscol and Crilly 2000). Chen (1975) and Nelson and Miller (1992) reported that the magnitude of swelling and shrinkage is an important factor in the safe and reliable design of foundations. There are many factors that govern the mechanism of swelling, e.g. amount and type of clay minerals, specific surface area, amount of non-expansive materials, dry unit weight, water content and the magnitude of surcharge pressure. Some researchers such as Abdullah et al. (1999), Alawaji (1999), Pusch (2001), Musso et al. (2003), Di Maio et al. (2004), Rao and Shivananda (2005) and Siddiqua et al. (2011) concluded from experimental tests that pore water quality influences the behaviour of expansive soils. Rao and Thyagaraj (2007a and 2007b), Li et al. (2014) and Estabragh et al. (2013 and 2015a) showed that the quality of inundating water also influences the swelling behaviour of soils.

Expansive soils are periodically exposed to cyclic drying and wetting in nature. Therefore, understanding the behaviour of expansive soils during cycles of drying and wetting is of great importance, particularly in arid and semi-arid regions. During cycles of drying and wetting the potential of swelling may decrease or increase. Dif and Bluemel (1991), Al-Homoud et al. (1995), Basma et al. (1996), Tripathy et al. (2002), Alonso et al. (2005), Estabragh et al. (2015b) and Soltani et al. (2017) indicated that the potential of swelling is reduced by increasing the number of cycles until it reaches a constant value. This behaviour was explained in the context of continuous rearrangement of soil particles.

On the contrary, some researchers such as Popescu (1979), Osipov et al. (1987) and Day (1994) have reported an opposite effect in which the magnitude of swelling is increased with the number of cycles. Cyclic drying and wetting of expansive soils can be conducted by controlling the suction (e.g. Wheeler et al. 2003; Alonso et al. 2005; Nowamooz and Masrouri 2008). Alonso et al. (2005) concluded from experimental results that the samples experience progressive irreversible deformation during drying and wetting until they reach a constant value. A review of the literature shows that the majority of research on cyclic drying and wetting has been done on samples with natural pore water and inundated with natural water. An exception is the work of Estabragh et al. (2013 and 2015a) who conducted experimental tests on samples with different quality of inundating water. Meanwhile, expansive soils can have a range of dissolved salt concentrations in their pore water (Rogers et al. 1994; Brady and Weil 1998). Pore water with different dissolved salt concentrations can be provided by natural or artificial causes such as infiltration of landfill leachate, infiltration from brine and chemical spillages from industrial operations (Barbour and Yang 1993; Rao and Shivananda 2005). The existing research works in the case of pore water quality are concentrated only on the swelling behaviour of expansive soils, while the mechanical properties of such soils have not been investigated during cycles of drying and wetting. Therefore, the main objective of this study is to investigate the effect of different pore water quality on the behaviour of an expansive soil during drying and wetting cycles. Experimental tests were conducted on samples prepared with different quality of pore water, i.e. distilled water, sodium chloride and calcium chloride solutions. Distilled water was used as the inundating water for all the samples during wetting. The results of this study will be presented in terms of vertical/radial deformation and void ratio–water content/suction shrink–swell paths.

2. Experimental work

2.1. *Materials*

2.1.1. Soil

A suitable soil to be used in this research work would be a highly expansive clay. Therefore, a number of kaolin–bentonite mixtures with different proportions were selected, and a series of samples were prepared according to the method that will be presented in the subsequent section. The swelling potential for the prepared samples was measured in accordance with the ASTM D4546-14 standard, and a suitable mixture with a high potential for swelling and shrinkage was chosen as per the classification criteria proposed by McKeen (1992). The chosen mixture was a mixture of 80% kaolin and 20% bentonite. Hereafter, this mixture will be simply referred to as soil. The physical, mechanical and chemical properties of the chosen mixture are provided in **Tables 1** and **2**. Based on the information provided in **Table 1**, the soil is classified as clay with high plasticity, i.e. CH, in accordance with the Unified Soil Classification System (USCS).

X-ray diffraction (XRD) tests were carried out on the samples of kaolin, bentonite and their mixture (i.e. 80% kaolin and 20% bentonite) to identify the mineralogical composition of the soils, and the results are shown in **Figures 1** and **2**. The minerals of kaolin include quartz, calcite, Na/Ca–feldspar, K–feldspar (see **Figure 1(a)**), and clay minerals group consisting of illite, chlorite and montmorillonite (see **Figure 2(a)**). **Figures 1(b)** and **2(b)** show that the minerals of bentonite consist of quartz, calcite, cristobalite, zeolite, dolomite, halite, and clay minerals group of illite and montmorillonite. The minerology of the chosen kaolin–bentonite mixture is similar to that of kaolin accounting for the addition and exclusion of K–feldspar and chlorite, respectively (see **Figures 1(c)** and **2(c)**).

2.1.2. Pore water and inundating water

Three types of liquids were used for preparing the samples: **i)** distilled water with pH=7.2 and electrical conductivity EC=0.14 dS/m; **ii)** 250 g/L sodium chloride solution (molar concentration M=4.28 mol/L) with pH=8.2 and EC=390 dS/m; and **iii)** 250 g/L calcium chloride solution (M=2.25 mol/L) with pH=9.3 and EC=390 ds/m. Distilled water was used for inundating the samples at various stages of the tests.

2.2. ***Sample preparation***

Standard Proctor compaction tests were carried out on the soil with different pore water quality, i.e. distilled water, 250 g/L NaCl and 250 g/L $CaCl_2$ solutions, in accordance with the ASTM D698-07 standard, and the compaction curves were established for all scenarios. For each pore water quality, samples for the cyclic drying and wetting tests were prepared at dry of optimum condition (i.e. approximately 5% less than the optimum water content and its corresponding dry unit weight; see points 1, 2 and 3 in **Figure 4**). The procedures that were used in preparing the different samples are as follows:

The required amount of liquid, either distilled water or salt solutions, corresponding to the desired water content (i.e. 5% less than the corresponding optimum water content) was added to the soil, and thoroughly mixed by hand. The moist mixtures were then kept in closed plastic bags and were allowed to cure for 24 hours. This allowed the moisture to evenly distribute throughout the soil mass. The static compaction technique was used for preparing the samples. Static compaction was done in a special mould by applying static pressure, using a loading machine (Estabragh et al. 2013). The dimensions of the mould was exactly the same as the oedometer ring, and was accommodated by detachable collars at both ends. Samples were prepared by static compaction of the moist soil in the mould in three layers. Each layer was compacted to a defined load at a fixed displacement rate of 1.5 mm/min until the desired dry unit weight was achieved (i.e. points 1, 2 and 3 in **Figure 4**). The load was the same for each layer, however, its value was dependent on the adopted pore water. The required load for each layer of the soil with a specific pore water was determined by trial and error. The values of applied load for each layer were 1190 kPa, 1528 kPa and 1530 kPa for samples with distilled water, NaCl and $CaCl_2$ solutions as the pore water. Prior placing the next layer, the surface of the compacted layer was scarified to ensure a good bond between adjacent layers of the sample. All samples were compacted in an identical fashion to provide the same dry unit weight and the same initial fabric in the samples.

2.3. *Apparatus and test procedure*

A conventional oedometer was modified to allow tests to be conducted under controlled temperature and surcharge pressure (Estabragh et al. 2013). This apparatus is similar to the one previously used by

Tripathy et al. (2002). The apparatus consists of a fixed ring with a modification to allow conducting shrinkage and swelling tests under controlled temperature and surcharge pressure as shown in **Figure 3** (Estabragh et al. 2013). Before starting the main tests, the apparatus was calibrated for temperature using a thermometer. The prepared soil sample with the desired pore water quality was placed in the ring between two porous stones with the load plate resting on the upper porous stone. The sample was loaded to a surcharge pressure of 10 kPa, and the pressure was maintained until full settlement was achieved. The sample was set at a temperature of 45°C. During heating, the water was gradually expelled from the sample and the volume of the sample decreased. The duration of this stage was about 7 days. The swelling stage was conducted by inundating the sample with distilled water, and the sample was allowed to swell under the same surcharge pressure of 10 kPa. The combination of one shrinkage and the subsequent swelling stage is denoted as a shrink–swell cycle. After wetting, a drying stage was implemented. The water flowed out from the cell by opening the drainage valve. the temperature controller was fixed at 45°C and the drying stage was repeated. The vertical deformation was recorded from the dial gauge readings during drying and wetting cycles. During drying, shrinkage of the soil sample caused the sample to decrease in diameter and height. Therefore, the volume change of the sample during the cycles of drying and wetting was three-dimensional. In order to plot the variations of void ratio with water content along a drying or wetting path within each cycle, at least six or seven duplicated samples of different pore water quality were tested for drying or wetting. The tests were performed in conventional oedometers. During the drying stage, the ring of the oedometer with the sample were transferred to an oven fixed at a temperature of 45°C with the same 10 kPa surcharge pressure as the main tests. The duplicated samples were dismantled at various stages, and further tested for height and diameter measurements. The diameter was measured at least in three points and the mean of the measurements was considered. The water content of each duplicated sample was also measured. Therefore, the variations of void ratio with water content during drying and wetting cycles was

determined by using the information from measuring the dimensions and corresponding water contents of the duplicated samples.

2.3.1. Chemical tests

At the end of each swelling stage, a 10 cm^3 sample of water was taken from the oedometer reservoir and was used to determine the pH and electrical conductivity EC of the inundating water. The duplicated samples (identical samples that were prepared with similar initial conditions as the main samples and subjected to drying and wetting) were dismantled using the ASTM procedure for extracting the pore water of the sample for measuring pH and EC.

2.3.2. Soil–water characteristic curve

The soil–water characteristic curve (SWCC) can be defined as the relationship between degree of saturation or water content (either gravimetric or volumetric) and soil suction (either total or matric). Determination of the SWCC is often done by the filter paper or pressure plate method. McQueen and Miller (1968) reported that the filter paper method can be used for measuring suctions ranging from a few kilopascals to several thousand kilopascals. It is possible to measure both the matric and total suctions by this method, so when the filter paper is not in contact with the sample the total suction is measured. The filter paper method was used according to the ASTM D5298-10 standard for measuring the matric suction of the samples with different pore water quality. The Whatman No. 42 filter paper was placed in contact with the sample in an airtight container for 7 days to achieve moisture equilibrium between the soil sample and the filter paper. Then by measuring the water content of the filter paper, the matric suction was determined by a calibration curve.

3. Results

The results of the compaction tests on samples with different pore water quality are shown in **Figure 4**. The maximum dry unit weight for the samples with distilled water, NaCl and $CaCl_2$ solutions were 16.0 kN/m^3, 16.9 kN/m^3 and 17.1 kN/m^3, respectively. The optimum water content for these samples was measured as 22.0%, 19.0% and 17.5%, respectively. As depicted in **Figure 4**, there is an increase in

maximum dry unit weight and a decrease in optimum water content for the samples with NaCl and $CaCl_2$ solutions compared to that of distilled water. The vertical deformation of the samples is expressed as the change in the height (ΔH) of the sample during either swelling or shrinkage as percentage of the initial height at the beginning of the first shrink–swell cycle. By plotting the vertical deformation of a sample for several shrink–swell cycles, the trend of variations in height of the sample during cycles of drying and wetting was observed. Variations of vertical deformation during cycles of drying and wetting for the samples prepared with different pore water quality is shown in **Figure 5**. The vertical deformation of the samples decreased during drying, which is due to thermo–hydro–mechanical (THM) coupling. The values of deformation for the samples with distilled water, NaCl and $CaCl_2$ solutions are 2.43%, 0.75% and 1.68%, respectively. These results show that the deformation for the sample with distilled water is more than those prepared with salt solutions. During wetting in this cycle, i.e. cycle 1, the vertical deformation was increased, which was observed as 12.08%, 12.70% and 13.00% for the samples with distilled water, NaCl and $CaCl_2$ solutions as the pore water, respectively. Therefore, the swelling potential is 14.51%, 13.45% and 14.68% for distilled water, NaCl and $CaCl_2$ solutions, respectively. By increasing the number of cycles, the potential of swelling and shrinkage is reduced. In cycle 3, for instance, the values of swelling potential for the samples were changed to 9.16%, 8.97% and 8.73% for distilled water, NaCl and $CaCl_2$ solutions, respectively. A comparison of these values with those in cycle 1 indicates that the swelling potential decreased by increasing the number of drying and wetting cycles. The swelling potential attained a nearly constant value with increasing the number of cycles (i.e. cycle 4). The deformations due to drying in the first cycle were 2.43%, 0.75% and 1.68% for distilled water, NaCl and $CaCl_2$ solutions, respectively. In the second cycle and due to THM coupling, the shrinkage potential was, respectively, changed to 9.04%, 9.33% and 8.38%. In the third cycle, these values were changed to 8.56%, 8.48% and 7.67%, and during the final cycle, i.e. cycle 4, they were further reduced to 7.80%, 7.85% and 7.26%, respectively. Therefore, the results show that the potential of deformation due to drying was reduced by increasing the number of cycles until it reached a nearly constant value. **Figure 6**

shows the variations of radial deformation during cycles of drying and wetting for the samples with different pore water quality. The information on the variations of radial deformation was obtained from the duplicated samples. In the first cycle of drying, the changes in radial deformation were 1.20%, 0.60% and 0.93% for distilled water, NaCl and $CaCl_2$ solutions, respectively. A comparison of these results with the vertical deformations at the same cycle (i.e. 2.43%, 0.75% and 1.68%, respectively) indicates that the radial deformations were less than the corresponding vertical deformations. During wetting, the radial deformation was reduced until it reached zero deformation condition (the same as the internal diameter of the oedometer ring). During the subsequent drying cycle, reduction in radial deformations occurred, so at the end of this stage they were 6.32%, 6.20% and 5.06% for distilled water, NaCl and $CaCl_2$ solutions, respectively. The results show that the radial deformation was decreased (similar to vertical deformation) until it reached a nearly constant value.

Typical results of void ratio versus water content, along with various constant saturation lines, for the samples prepared with NaCl solution as the pore water are shown in **Figures 7(a)–7(d)**. In these figures, the changes of void ratio e with water content w is shown from the initial (as compacted) condition to the fourth cycle of drying and wetting. Points B, D, F and H show the position of the samples at the end of shrinkage (drying) stages in different cycles, while points C, E, G and I indicate the position of the samples at the end of swelling (wetting) stages. Point A in **Figure 7(a)** shows the initial or as compacted void ratio and water content of the sample. In the first cycle, drying occurred from point A to B followed by wetting from point B to C (see **Figure 7(a)**). It is resulted from **Figure 7** that the soil reached nearly full saturation in all stages of wetting, and that all the drying and wetting curves were *S*–shaped. The tendency to converge to the same *S*–shaped curve was evolved by repeating the cycles of drying and wetting. **Figure 8** illustrates void ratio–water content shrink–swell paths at equilibrium condition for the samples with different pore water quality. As shown in this figure, the paths of drying and wetting for the samples with NaCl and $CaCl_2$ solutions nearly coincide with each other.

Figure 9 shows the soil–water characteristic curve for the samples with different pore water quality. Villar (1995), Alonso et al. (2005) and Estabragh et al. (2013) expressed the variation of water content with suction using a linear relationship. In the present study, an attempt was made to find the best-fit relationship and hence the following relationship was proposed:

$$w = a + b\exp(-cS) \quad (1)$$

where w=water content (in %); S=suction (in kPa); and a, b and c=fitting parameters which are dependent on pore water quality. The values of the fitting parameters for different pore water quality are as follows: **i)** a=1.638, b=35.36 and c=9.22×10^{-5} for distilled water; **ii)** a=0.011, b=45.56 and c=4.36×10^{-5} for NaCl solution; and **iii)** a=0.785, b=42.78 and c=4.72×10^{-5} for $CaCl_2$ solution.

By using **Equation (1)**, it is possible to relate water content (as shown in **Figure 7**) to suction, and hence find the corresponding relationship between void ratio and suction for a given pore water quality.

4. Discussion

The surfaces of clay particles carry unbalanced negative charges in dry or wet condition. They attract cations (positive ions) that are tightly attached to the clay surface. In addition to the cations needed to neutralize the electrical charge on the clay surface, there are some salt precipitates comprising of a combination of cations and anions. By adding water to the soil, these ions go into solution. Desorption of cations from the clay surface leads to a higher concentration of cations near the clay surface, which promotes a tendency among cations to diffuse away. This tendency for diffusion, however, is restricted by the attractive forces between the cations and the surface of the negatively charged clay particle. The outcome of these opposing actions promotes the development of an ion distribution in the vicinity of the clay particle. This system of distributed ions along with the negatively charged surface of the clay is termed as the diffuse double layer or DDL (Mitchell and Soga 2005). Changes in the thickness of the DDL can lead to different fabric of soil. The isomorphous substitution phenomenon may occur in clay soils where the cations can be attached to the surface of the clay. These are termed as exchange cations, since they can be changed with other cations. The replacement of one type of cation by another depends

on many factors such as valence and ion size. The cations of higher valance are adsorbed on the clay surface with a higher force compared with the cations of lower valance.

Bowders and Daniel (1987) and Abdullah et al. (1999) reported that many chemical solutions tend to reduce the thickness of the DDL, thereby reducing the repulsive forces among particles and thus forming a flocculated soil fabric. Musso et al. (2003) indicated that changes in the chemical composition of the pore fluid have different effects on clay soils. They reported that these effects can be exchanges of cations between the mineralogical units or variations in the electro-chemical forces acting between different platelets, and variations in osmotic pressure. The results of the compaction tests for the samples with NaCl and $CaCl_2$ solutions as the pore water showed that the maximum dry unit weight increased (i.e. 16.9 kN/m^3 and 17.1 kN/m^3, respectively) and the optimum water content decreased (i.e. 19.0% and 17.5%, respectively) in comparison to that of distilled pore water (i.e. 16.0 kN/m^3 and 22.0%). This change in maximum dry unit weight and optimum water content can be resulted from reduction in the thickness of the DDL surrounding the clay particles. The reduction of the DDL thickness brings the particles closer, and decreases the water holding capacity that causes the optimum water content to decrease.

The results in **Figure 5** shows that the vertical deformation upon the first drying cycle is greater for distilled pore water than that of NaCl and $CaCl_2$ solutions, and that for the sample with NaCl it is less than $CaCl_2$. This can be explained with aid from the DDL concept. As it was discussed above, the effect of chemical solutions can change the thickness of the DDL, which may result in particles being pasted to each other leading to coarser particles. The results of the compaction tests for samples with salt solutions also showed that the maximum dry unit weight and optimum water content, respectively, increased and decreased in comparison with distilled water. These variations indicate reduction in thickness of the DDL. The thickness of the DDL is dependent on factors such as valence and concentration of the cations (Mitchell and Soga 2005). Comparing the results for NaCl and $CaCl_2$ solutions indicates that the effect of NaCl in reduction of the deformation due to drying in the first cycle is less than $CaCl_2$ and distilled water. During drying or wetting, the surcharge pressure was the same for all samples with different pore water

quality. By adding NaCl solution for preparing the sample, the processes of exchange of ions increase the attractive forces and leads to reduction of the DDL thickness, and thus a structure for the soil is formed with low void ratio. In the case of $CaCl_2$, the processes of exchange of ions also leads to reduction of the DDL thickness; however, it is not the same as the effect of NaCl, since more sodium ions may be adsorbed to the clay particle compared with calcium ions. Therefore, for the samples prepared with $CaCl_2$ solution, the degree of flocculation is less and the void ratio between particles is more compared with the samples prepared with NaCl. This results in more deformation under constant load for the pore fluid with $CaCl_2$ than with NaCl. A comparison of the results for the samples with NaCl and $CaCl_2$ solutions indicated that the effect of NaCl in reducing the deformation due to drying is less than $CaCl_2$. This indicates that the effect of NaCl in shrinking the DDL is more than $CaCl_2$. The subsequent wetting stage in this cycle showed that the swelling potentials for samples with NaCl and $CaCl_2$ solutions are 13.45% and 14.67%, respectively. This shows that the swelling potential of the sample with $CaCl_2$ solution is more than that of NaCl. This is probably because, during wetting, the bonding that was created between the particles during sample preparation and drying breaks more in the presence of $CaCl_2$ compared to NaCl. The mechanism of swelling can be explained as follows:

Expansive soils are generally in unsaturated condition due to desiccation. They have two components of suction, namely matric suction S and osmotic suction π. Matric suction can be considered as the negative pore water pressure due to surface tension effects. Osmotic suction results from the dissolved salt concentration in the pore fluid of the sample. Prior inundation, the sample is in unsaturated condition. Upon inundating the sample, water flows from the reservoir to the sample and the initial matric suction is gradually reduced until full saturation is attained. The osmotic suction appears in the sample after saturation. Water follows to the sample due to osmotic suction, thereby increasing the pore water pressure in the sample. The following relationship can be used to describe the effect of variations of pore water pressure:

$$\sigma' = \sigma - u_w \quad (2)$$

where σ'=effective stress; σ=acting surcharge pressure on the sample that is constant during the test (=10 kPa in this study); and u_w=pore water pressure the changes of which can be due to osmotic suction. Therefore, for a constant σ, an increase in u_w results in a decrease in σ', which causes changes in the thickness and ion concentration of the DDL. As a result, swelling occurs in the sample.

The chemical test results, i.e. pH and electrical conductivity EC, of the liquid samples taken from the reservoir water and extracted from pore water of the duplicated samples at the end of each cycle are presented in **Tables 3**, **4** and **5** for distilled water, NaCl and $CaCl_2$ solutions, respectively. As shown in **Table 3**, the values of pH and EC for both the reservoir water and extracted pore water decreased from their values at the end of the first cycle (e.g. EC decreased from 3.52 dS/m at the end of the first cycle to 1.80 dS/m at the end of the fifth cycle for the reservoir water). A similar yet more pronounced decreasing trend can also be seen in **Tables 4** and **5** for the samples containing NaCl and $CaCl_2$ solutions as the pore water. Based on the results presented in **Tables 3**, **4** and **5**, it can be concluded that migration of salt from the samples to the reservoir has occurred. After the first cycle, the subsequent cycle begun with drying. In this case, the potential of drying was increased in comparison with that observed in the first cycle. It can be said that after wetting in the first cycle, the pores between the particles were increased and during drying, since the volume of solids is constant, the volume of pores was reduced and caused an increase in the potential of drying. This can be due to the increase in the spaces between particles during swelling due to repulsive forces. The amount of shrinkage during drying is more for NaCl solution than the other solutions. These findings are in agreement with the results that were reported by Dif and Bluemel (1991), Day (1994), Al-Homoud et al. (1995), Tripathy et al. (2002), Subba Rao and Tripathy (2003) and Alonso et al. (2005). On the other hand, other researchers such as Chu and Mou (1973) have reported an opposite effect in which the swelling potential increased with the number of successive cycles. All these tests show that elastic equilibrium can be attained at the end of several cycles. This can be attributed to the reconstruction of the clay micro-structure upon completion of the first or second cycle (Dif and Bluemel

1991; Sridharan and Allam 1982). Bell (1992) suggested that repeated wetting and drying can cause aggregation of soil particles in residual soils. According to Bell's suggestion, drying initiates cementation by formation of aggregation, leading to some relatively large inter-pores formed between the aggregated soil lumps. These large inter-pores reduce the soil's absorption rate along a certain range of wetting paths. At equilibrium condition, the micro-structure becomes even more uniform in nature, thus ensuring lesser water absorption resulting in lesser swelling. This inevitably causes a reduction in the magnitude of swelling and shrinkage compared with the first and second cycles (Zhang et al. 2006).

It is generally known that clay soils can crack during drying. Cracks occur when the tensile stresses developed within the soil due to drying exceed the tensile strength of the soil. Tensile stresses develop only when the soil is restrained in some way against shrinkage (Kodikara et al. 2000). The formation and development of cracks is enhanced by the availability of clay (Mitchell and Soga 2005). In high plasticity soils, self-healing may result in closing up of cracks during wetting. The determination of the crack dimensions is an important factor in understanding the behaviour of expansive soils as it affects, for instance, hydraulic conductivity and variations of void ratio with water content. There is no standard method for measuring the crack dimensions at the end of drying. Image processing techniques have been suggested by some researchers such as Peng et al. (2006). Rayhani et al. (2008) used a digital calliper for measuring the length and width of the cracks. In this work, the existence of cracks was examined using the duplicated samples. At the end of drying for various cycles a few surface cracks were observed. The average depth of these cracks were less than 1.0 mm. The extension of the cracks was reduced by increasing the cycles. Since the number of the cracks were not considerable, no measurements was taken. Researchers such as Dif and Bluemel (1991), Al-Homoud et al. (1995), Basma et al. (1996), Subba Rao et al. (2000) and Tripathey et al. (2002) who have worked on studying the behaviour of soils during cycles of wetting and drying did not report the existence of any cracks at the end of drying stages.

It is resulted from comparing the vertical and radial deformations (compare **Figures 5** and **6**) that the radial deformations are less than the corresponding vertical deformations at different cycles of drying and

wetting. By increasing the number of drying and wetting cycles, the radial deformations are decreased similar to that observed for the vertical deformations. Tang et al. (2008) defined the isotropic condition as a condition where the vertical and radial strains are equal for the sample during deformation. Based on the obtained results in this work, it is concluded that the soil samples had an anisotropic behaviour.

As typically shown in **Figure 7**, all of the samples reached nearly full saturation during the wetting stages and during drying they gradually moved away from the full saturation line and became more unsaturated, resulting in reduction of water content and very small changes in void ratio. The drying continued until the degree of saturation was less than 40%. The results show that all of the drying and wetting curves are *S*–shaped, and thus consist of three sections, i.e. two curvilinear portions at the top and bottom, and a linear portion in the middle. The variations of void ratio and water content at the top and bottom of the *S*–shaped curve are insignificant. The middle section of the curve, however, is linear and nearly parallel with the full saturation line with high variations of void ratio and water content. A comparison of the results in **Figures 7(a)–7(d)** shows that the distance between the drying and wetting curves is decreased by increasing the number of drying and wetting cycles. **Figure 8** illustrates void ratio–water content paths for the samples with different pore water quality at equilibrium condition. It is shown that the drying and wetting curves coincide, and thus can be represented by a unique *S*–shaped curve. These results are in agreement with the results that were reported by Hanafy (1991) and Tripathy et al. (2002). All of the curves are similar in shape (all are *S*–shaped), and the curves for NaCl and $CaCl_2$ solutions nearly coincide with each other. However, the curve for distilled water is located above the other two at a considerable distance. The difference between the positions of the void ratio–water content curves for the samples prepared with distilled water and those prepared with salt solutions (see **Figure 8**) can be attributed to the difference in thickness of the DDL in these samples. As shown in **Figure 8**, the linear portion of these curves are not ideally parallel to the line of 100% saturation, and they are located within the saturation degrees of 60% and 90% at equilibrium condition.

It is resulted from **Figure 9** (the soil–water characteristic curves) that for a specific water content, particularly for water contents less than 25%, the matric suction for the samples prepared with distilled water is less than those prepared with salt solutions. As mentioned above, the total suction of a soil is composed of two components, i.e. matric suction and osmotic suction. Changes in total suction can be caused by a change in either one or both components of the suction. The osmotic suction for the samples with NaCl and $CaCl_2$ solutions is more than that of distilled water. Therefore, the total suction of the samples with NaCl and $CaCl_2$ is more than the sample with distilled water. This increase is resulted from increases in both the osmotic and matric suctions, however, the contribution of increasing matric suction is more than osmotic suction. Using data from different soils Fredlund et al. (2012) reported that an increase in total suction causes a greater increase in matric suction compared to osmotic suction. This could explain the increase in matric suction for the samples prepared with salt solutions compared to those prepared with distilled water.

The hysteresis phenomenon is a behaviour where a soil having the same water contents corresponding to drying and wetting paths does not have the same suction. Differences in the contact angles during drying and wetting can be the reason of hysteresis (Dineen 1997). Fredlund et al. (2012) considered the hysteresis to be due to the existence of entrapped air in the soil. Yong and Warkentin (1975) explained the hysteresis phenomenon in terms of the ink–bottle effect for granular soils. Hysteresis for soils is often explained with the soil–water characteristic curve. Many researchers have attempted to correlate some other hydraulic or mechanical properties of unsaturated soils with the water retention behaviour (Fredlund et al. 2012). However, it should be noted that the water retention behaviour is significantly influenced by the void ratio of unsaturated soils (Gallipoli et al. 2003). Changes in void ratio has an important effect on the position of the main drying and wetting curves. Therefore, the soil–water characteristic curve is significantly affected by changes in void ratio. Kawai et al. (2000), Romero and Vaunat (2000), Gallipoli et al. (2003) and Wheeler et al. (2003) proposed equations for the soil–water characteristic curve that include the void ratio of the soil. Based on **Equation (1)** and the information which was partially

illustrated in **Figure 7**, the variations of void ratio with suction was established during drying and wetting cycles for the samples with different pore water quality. Typical void ratio–suction shrink–swell paths at the first cycle for the sample with distilled pore water is shown in **Figure 10(a)**. In addition, **Figure 10(b)** illustrates void ratio–suction paths for the samples with different pore water quality at equilibrium condition. As shown in **Figure 10(a)**, the variations of void ratio and suction are not the same for the first cycle of drying and wetting. However, at the final cycle the paths of drying and wetting nearly coincide with each other, and thus can be represented by a unique curve (see **Figure 10(b)**). It is resulted that when the samples attain equilibrium condition the effect of hysteresis is eliminated. Therefore, at equilibrium condition not only the plastic deformations but also the hysteresis are diminished.

Expansive soils often exhibit volume change upon drying and/or wetting due to variations in water content. The volume change can cause extensive damage to structures, particularly light buildings and pavements. There are different methods to reduce the volume change potential of these soils, i.e. chemical and mechanical techniques. The results of this work indicate that it is possible to reduce the potential of volume change in expansive soils by conducting drying and wetting periodically. This method has many advantages including the ease of implementation and lower cost in comparison with other methods. Laboratory tests should be conducted on samples to find the suitable duration of drying and wetting for different expansive soils and pore water qualities.

5. Conclusions

Cyclic drying and wetting tests were performed on samples of an expansive soil prepared with different pore water quality, and inundated with distilled water. The following conclusions can be drawn from the results of this work:

1. Plastic deformation was observed during drying and wetting for samples with different pore water quality. The irreversible deformation diminished after three or four cycles when the equilibrium condition was achieved.

2. During the initial cycles of drying and wetting, the potential of shrinking and swelling is dependent on the pore water quality; however, by increasing the number of cycles they reach the same value for different quality of pore water.
3. The drying and wetting paths in the space of void ratio and water content are *S*–shaped curves. Each *S*–shaped curve consists of one linear and two curvilinear portions. For the samples with salt solutions as the pore water, these curves nearly coincide with each other at equilibrium condition, and the reduction in volume of them is more compared to the samples with distilled pore water. The drying and wetting curves for the samples with salt solutions are closer to the 100% saturation line compared to the sample with distilled pore water. The majority of the sample's volume change was observed in the linear section of the *S*–shaped curve.
4. The shape of the soil–water characteristic curve (SWCC) is dependent on the pore water quality of the soil sample. The hysteresis phenomenon is seen during drying and wetting cycles, and it is eliminated by increasing the number of cycles.

References

Abdullah, W. S., Alshibli, K. A., & Al-Zou'bi, M. S. **(1999)**. Influence of pore water chemistry on the swelling behavior of compacted clays. *Applied Clay Science*, *15*(5–6), 447–462. http://doi.org/10.1016/s0169-1317(99)00034-4

Alawaji, H. A. **(1999)**. Swell and compressibility characteristics of sand–bentonite mixtures inundated with liquids. *Applied Clay Science*, *15*(3–4), 411–430. http://doi.org/10.1016/s0169-1317(99)00033-2

Al-Homoud, A. S., Basma, A. A., Malkawi, A. I. H., & Al-Bashabsheh, M. A. **(1995)**. Cyclic swelling behaviour of clays. *Journal of Geotechnical Engineering*, *121*(7), 562–565. http://doi.org/10.1061/(asce)0733-9410(1995)121:7(562)

Alonso, E. E., Romero, E., Hoffmann, C., & García-Escudero, E. **(2005)**. Expansive bentonite–sand mixtures in cyclic controlled–suction drying and wetting. *Engineering Geology*, *81*(3), 213–226. http://doi.org/10.1016/j.enggeo.2005.06.009

Barbour, S. L., & Yang, N. **(1993)**. A review of the influence of clay–brine interactions on the geotechnical properties of Ca–montmorillonitic clayey soils from western Canada. *Canadian Geotechnical Journal*, *30*(6), 920–934. http://doi.org/10.1139/t93-090

Basma, A. A., Al-Homoud, A. S., Malkawi, A. I. H., & Al-Bashabsheh, M. A. **(1996)**. Swelling–shrinkage behavior of natural expansive clays. *Applied Clay Science*, *11*(2–4), 211–227. http://doi.org/10.1016/s0169-1317(96)00009-9

Bell, F. G. **(1992)**. Cohesive soils. In *Engineering properties of soils and rocks* (pp. 36–84). Woburn: Butterworth–Heinemann Ltd. http://doi.org/10.1016/b978-0-7506-0489-5.50006-8

Bowders Jr., J. J., & Daniel, D. E. **(1987)**. Hydraulic conductivity of compacted clay to dilute organic chemicals. *Journal of Geotechnical Engineering*, *113*(12), 1432–1448. http://doi.org/10.1061/(asce)0733-9410(1987)113:12(1432)

Brady, N. C., & Weil, R. R. **(1998)**. *Nature and properties of soils* (12th Ed.). Upper Saddle River, NJ: Prentice Hall Inc. ISBN 9780138524449

Chen, F. H. **(1975)**. Foundations on expansive soils (1st Ed.). Amsterdam: Elsevier Scientific Publication Co. ISBN 0444413936

Chu, T. Y., & Mou, C. H. **(1973)**. Volume change characteristics of expansive soils determined by controlled suction. In *Proceeding of the 3rd International Conference on Expansive Soils* (pp. 177–185). Jerusalem: Academic Press.

Day, R. W. **(1994)**. Swell–shrink behaviour of compacted clay. *Journal of Geotechnical Engineering*, *120*(3), 618–623. http://doi.org/10.1061/(asce)0733-9410(1994)120:3(618)

Di Maio, C., Santoli, L., & Schiavone, P. **(2004)**. Volume change behaviour of clays: The influence of mineral composition, pore fluid composition and stress. *Mechanics of Materials*, *36*(5–6), 435–451. http://doi.org/10.1016/s0167-6636(03)00070-x

Dif, A., & Bluemel, W. **(1991)**. Expansive soils under cyclic drying and wetting. *Geotechnical Testing Journal*, *14*(1), 96–102. http://doi.org/10.1520/gtj10196j

Dineen, K. **(1997)**. *The influence of soil suction on compressibility and swelling*. PhD dissertation (858 p.), Imperial College, University of London, UK.

Driscoll, R. M. C., & Crilly, M. S. **(2000)**. *Subsidence damage to domestic buildings: Lessons learned and questions remaining* (1st Ed.). Watford: CRC Press. ISBN 1860814336

Estabragh, A. R., Moghadas, M., & Javadi, A. A. **(2013)**. Effect of different types of wetting fluids on the behaviour of expansive soil during wetting and drying. *Soils and Foundations*, *53*(5), 617–627. http://doi.org/10.1016/j.sandf.2013.08.001

Estabragh, A. R., Moghadas, M., & Javadi, A. A. **(2015a)**. Mechanical behaviour of an expansive clay mixture during cycles of wetting and drying inundated with different quality of water. *European Journal of Environmental and Civil Engineering*, *19*(3), 278–289. http://doi.org/10.1080/19648189.2014.960098

Estabragh, A. R., Parsaei, B., & Javadi, A. A. **(2015b)**. Laboratory investigation of the effect of cyclic wetting and drying on the behaviour of an expansive soil. *Soils and Foundations*, *55*(2), 304–314. http://doi.org/10.1016/j.sandf.2015.02.007

Fredlund, D. G., Rahardjo, H., & Fredlund, M. D. **(2012)**. *Unsaturated soil mechanics in engineering practice* (2nd Ed.). Hoboken: John Wiley & Sons. http://doi.org/10.1002/9781118280492, ISBN 9781118133590

Gallipoli, D., Wheeler, S. J., & Karstunen, M. **(2003)**. Modelling the variation of degree of saturation in a deformable unsaturated soil. *Géotechnique*, *53*(1), 105–112. http://doi.org/10.1680/geot.2003.53.1.105

Gourley, C. S., Newill, D., & Schreiner, H. D. **(1994)**. Expansive soils: TRL's research strategy. In P. G. Fookes & R. H. G. Parry (Eds.), *Proceedings of the 1st International Symposium on Engineering Characteristics of Arid Soils* (pp. 247–260). Rotterdam: A.A. Balkema. ISBN 9054103655

Hanafy, E. A. D. E. **(1991)**. Swelling/Shrinkage characteristic curve of desiccated expansive clays. *Geotechnical Testing Journal*, *14*(2), 206–211. http://doi.org/10.1520/gtj10562j

Kawai, K., Karube, D., & Kato, S. **(2000)**. The model of water retention curve considering effects of void ratio. In H. Rahardjo, D. G. Toll, & E. C. Leong (Eds.), *Proceedings of the 1st Asian Conference on Unsaturated Soils* (pp. 329–334). Rotterdam: A.A. Balkema. ISBN 9058091992

Kodikara, J. K., Barbour, S. L., & Fredlund, D. G. **(2000)**. Desiccation cracking of soil layers. In H. Rahardjo, D. G. Toll, & E. C. Leong (Eds.), *Proceedings of the 1st Asian Conference on Unsaturated Soils* (pp. 693–698). Rotterdam: A.A. Balkema. ISBN 9058091992

Li, Z., Tang, C., Hu, R., & Zhou, Y. **(2014)**. Experimental research on expansion characteristics of Mengzi expansive soil with water, salt and acid immersion. *Environmental Earth Sciences*, *72*(2), 363–371. http://doi.org/10.1007/s12665-013-2957-z

McKeen, R. G. **(1992)**. A model for predicting expansive soil behavior. In *Proceedings of the 7th International Congress on Expansive Soils* (pp. 1–6). Dallas, Texas, USA.

McQueen, I. S., & Miller, R. F. **(1968)**. Calibration and evaluation of wide range method of measuring moisture stress. *Soil Science*, *106*(3), 225–231. http://doi.org/10.1097/00010694-196809000-00012

Mitchell, J. K., & Soga, K. **(2005)**. Soil–water–chemical interactions. In *Fundamentals of soil behavior* (3rd Ed., pp. 143–172). Hoboken: John Wiley & Sons. http://doi.org/10.2136/sssaj1976.03615995004000040003x, ISBN 9780471463023

Musso, G., Morales, E. R., Gens, A., & Castellanos, E. **(2003)**. The role of structure in the chemically induced deformations of FEBEX bentonite. *Applied Clay Science*, *23*(1–4), 229–237. http://doi.org/10.1016/s0169-1317(03)00107-8

Nelson, J. D., & Miller, D. J. **(1992)**. *Expansive soils: Problems and practice in foundation and pavement engineering* (1st Ed.). New York: John Wiley & Sons. ISBN 0471511862

Nowamooz, H., & Masrouri, F. **(2008)**. Hydromechanical behaviour of an expansive bentonite/silt mixture in cyclic suction–controlled drying and wetting tests. *Engineering Geology*, *101*(3–4), 154–164. http://doi.org/10.1016/j.enggeo.2008.04.011

Osipov, V. I., Bik, N. N., & Rumjantseva, N. A. **(1987)**. Cyclic swelling of clays. *Applied Clay Science*, *2*(4), 363–374. http://doi.org/10.1016/0169-1317(87)90042-1

Peng, X., Horn, R., Peth, S., & Smucker, A. **(2006)**. Quantification of soil shrinkage in 2D by digital image processing of soil surface. *Soil and Tillage Research*, *91*(1–2), 173–180. http://doi.org/10.1016/j.still.2005.12.012

Popescu, M. E. **(1979)**. Engineering problems associated with expansive clays from Romania. *Engineering Geology*, *14*(1), 43–53. http://doi.org/10.1016/0013-7952(79)90062-0

Pusch, R. **(2001)**. *Experimental study of the effect of high pore water salinity on the physical properties of a natural smectite clay*. Technical Report No. TR01–07 (35 p.), Swedish Nuclear Fuel and Waste Management Co., Stockholm, Sweden. ISSN 14040344

Rao, S. M., & Shivananda, P. **(2005)**. Role of osmotic suction in swelling of salt–amended clays. *Canadian Geotechnical Journal*, *42*(1), 307–315. http://doi.org/10.1139/t04-086

Rao, S. M., & Thyagaraj, T. **(2007a)**. Role of direction of salt migration on the swelling behaviour of compacted clays. *Applied Clay Science*, *38*(1–2), 113–129. http://doi.org/10.1016/j.clay.2007.02.005

Rao, S. M., & Thyagaraj, T. **(2007b)**. Swell–compression behaviour of compacted clays under chemical gradients. *Canadian Geotechnical Journal*, *44*(5), 520–532. http://doi.org/10.1139/t07-002

Rayhani, M. H. T., Yanful, E. K., & Fakher, A. **(2008)**. Physical modeling of desiccation cracking in plastic soils. *Engineering Geology*, *97*(1–2), 25–31. http://doi.org/10.1016/j.enggeo.2007.11.003

Rogers, C. D. F., Dijkstra, T. A., & Smalley, I. J. **(1994)**. Classification of arid soils for engineering purposes: An engineering approach. In P. G. Fookes & R. H. G. Parry (Eds.), *Proceeding of the 1st International Symposium on Engineering Characteristics of Arid Soils* (pp. 99–134). Rotterdam: A.A. Balkema. ISBN 9054103655

Romero, E., & Vaunat, J. **(2000)**. Retention curves in deformable clays. In A. Tarantino & C. Mancuso (Eds.), *Experimental Evidence and Theoretical Approaches in Unsaturated Soils* (pp. 91–106). Rotterdam: A.A. Balkema. ISBN 9058091864

Siddiqua, S., Blatz, J., & Siemens, G. **(2011)**. Evaluation of the impact of pore fluid chemistry on the hydromechanical behaviour of clay–based sealing materials. *Canadian Geotechnical Journal*, *48*(2), 199–213. http://doi.org/10.1139/t10-064

Soltani, A., Taheri, A., Khatibi, M., & Estabragh, A. R. **(2017)**. Swelling potential of a stabilized expansive soil: A comparative experimental study. *Geotechnical and Geological Engineering*, *35*(4), 1717–1744. http://doi.org/10.1007/s10706-017-0204-1

Sridharan, A., & Allam, M. M. **(1982)**. Volume change behavior of desiccated soils. *Journal of the Geotechnical Engineering Division*, *108*(8), 1057–1071. http://doi.org/10.1016/0148-9062(83)91686-8

Subba Rao, K. S., & Tripathy, S. (**2003**). Effect of aging on swelling and swell–shrink behaviour of a compacted expansive soil. *Geotechnical Testing Journal*, *26*(1), 36–46. http://doi.org/10.1520/gtj11100j

Subba Rao, K. S., Rao, S. M., & Gangadhara, S. **(2000)**. Swelling behavior of a desiccated clay. *Geotechnical Testing Journal*, *23*(2), 193–198. http://doi.org/10.1520/gtj11043j

Tang, A. M., Cui, Y. J., & Barnel, N. **(2008)**. Thermo–mechanical behaviour of a compacted swelling clay. *Géotechnique*, *58*(1), 45–54. http://doi.org/10.1680/geot.2008.58.1.45

Tripathy, S., Subba Rao, K. S., & Fredlund, D. G. (**2002**). Water content–void ratio swell–shrink paths of compacted expansive soils. *Canadian Geotechnical Journal*, *39*(4), 938–959. http://doi.org/10.1139/t02-022

Villar, M. V. **(1995)**. First results of suction controlled oedometer test in highly expansive montmorillonite. In E. E. Alonso & P. Delage (Eds.), *Proceeding of the 1st International Conference on Unsaturated Soils* (pp. 207–213). Rotterdam: A.A. Balkema. ISBN 9054105836

Wheeler, S. J., Sharm, R. S., & Buisson, M. S. R. **(2003)**. Coupling of hydraulic hysteresis and stress–strain behaviour in unsaturated soils. *Géotechnique*, *53*(1), 41–54. http://doi.org/10.1680/geot.2003.53.1.41

Yong, R. N., & Warkentin, B. P. **(1975)**. *Soil properties and behaviour* (1st Ed.). Amsterdam: Elsevier Scientific Publication Co. ISBN 9780444601360

Zhang, R., Yang, H., & Zheng, J. **(2006)**. The effect of vertical pressure on the deformation and strength of expansive soil during cyclic wetting and drying. In G. A. Miller, C. E. Zapata, S. L. Houston, & D. G. Fredlund (Eds.), *Proceedings of the 4th International Conference on Unsaturated Soils* (pp. 894–905). Carefree: ASCE. http://doi.org/10.1061/40802(189)71

List of Tables

Table 1. Physical and mechanical properties of the used soil.

Properties	**Value**
Specific gravity, G_s	2.75
Grain–size distribution	
Gravel (%)	0.0
Sand (%)	26.0
Silt and Clay (%)	74.0
Consistency limits	
Liquid limit, *LL* (%)	81.0
Plastic limit, *PL* (%)	27.5
Plasticity index, *PI* (%)	53.5
USCS classification	CH
Compaction characteristics	
Optimum water content, w_{opt} (%)	16.0
Maximum dry unit weight, γ_{dmax} (kN/m^3)	22.0

Table 2. Chemical composition of the used soil.

Chemical components	**Amount**
pH	8.4
EC* (dS/m)	13.9
Na^+ (meq/L)	142.0
Ca^{2+} (meq/L)	21.0
Mg^{2+} (meq/L)	6.0
Cl^- (meq/L)	49.0
HCO_3^- (meq/L)	7.5
SO_4^{2-} (meq/L)	112.0

* Electrical conductivity.

Table 3. Chemical composition of the extracted pore water and the reservoir water at the end of each cycle for the sample with distilled water as the pore water.

Condition	**Extracted pore water**		**Reservoir water**	
Number of cycle	**pH**	**EC[*] (dS/m)**	**pH**	**EC (dS/m)**
1	7.9	9.17	7.8	3.52
2	8.1	6.33	6.2	2.38
3	7.9	7.25	5.4	1.98
4	8.2	5.00	6.5	1.81
5	8.0	8.12	6.4	1.80

[*] Electrical conductivity.

Table 4. Chemical composition of the extracted pore water and the reservoir water at the end of each cycle for the sample with NaCl solution as the pore water.

Condition	**Extracted pore water**		**Reservoir water**	
Number of cycle	**pH**	**EC[*] (dS/m)**	**pH**	**EC (dS/m)**
1	7.9	12.24	7.4	17.67
2	8.0	6.31	7.8	4.97
3	8.1	3.42	8.1	3.39
4	8.0	3.20	8.0	3.31

[*] Electrical conductivity.

Table 5. Chemical composition of the extracted pore water and the reservoir water at the end of each cycle for the sample with $CaCl_2$ solution as the pore water.

Condition	**Extracted pore water**		**Reservoir water**	
Number of cycle	**pH**	**EC[*] (dS/m)**	**pH**	**EC (dS/m)**
1	7.5	24.40	7.1	11.40
2	7.8	9.11	6.6	11.61
3	7.8	8.16	7.1	8.87
4	7.4	7.90	7.0	8.72

[*] Electrical conductivity.

List of Figures

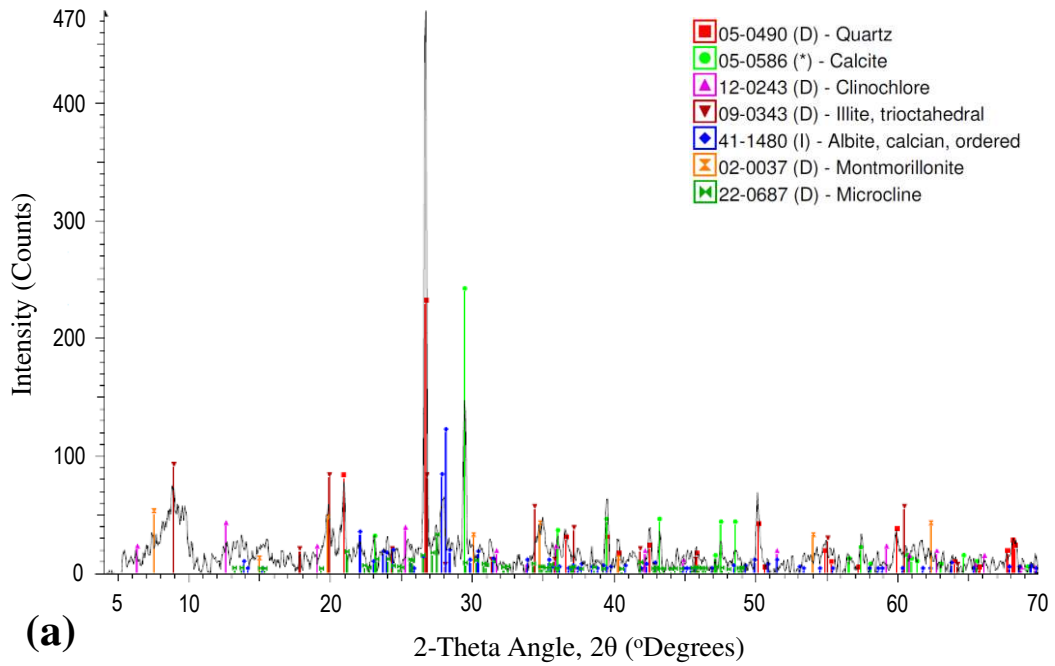
05-0490 (D) - Quartz
05-0586 (*) - Calcite
12-0243 (D) - Clinochlore
09-0343 (D) - Illite, trioctahedral
41-1480 (I) - Albite, calcian, ordered
02-0037 (D) - Montmorillonite
22-0687 (D) - Microcline
Intensity (Counts)
2-Theta Angle, 2θ (°Degrees)

(a)

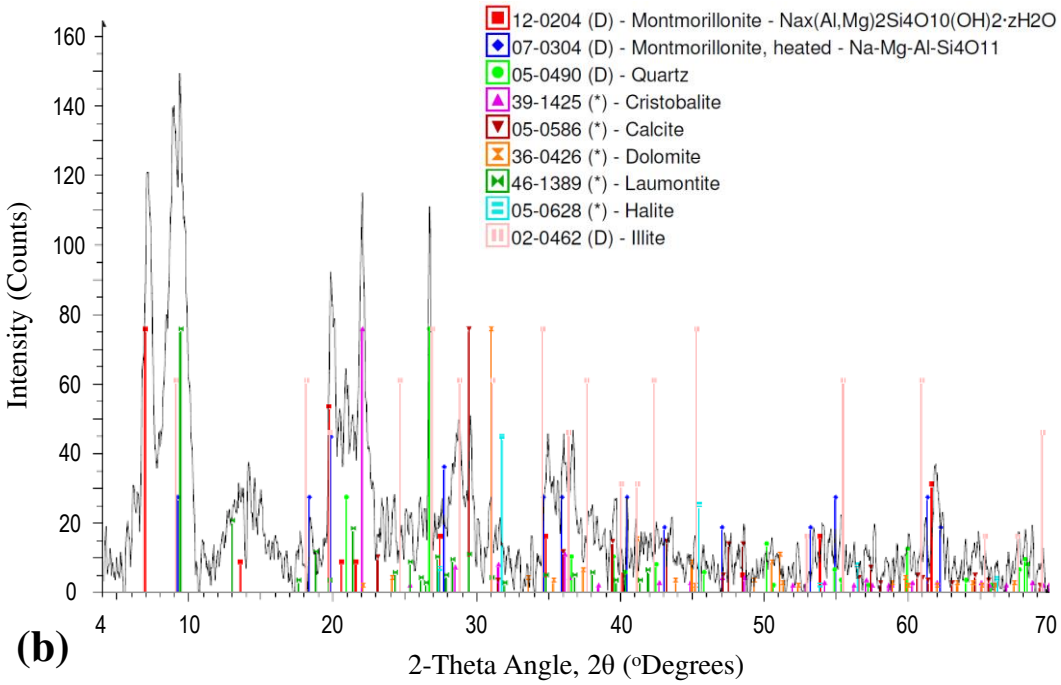
12-0204 (D) - Montmorillonite - Nax(Al,Mg)2Si4O10(OH)2·zH2O
07-0304 (D) - Montmorillonite, heated - Na-Mg-Al-Si4O11
05-0490 (D) - Quartz
39-1425 (*) - Cristobalite
05-0586 (*) - Calcite
36-0426 (*) - Dolomite
46-1389 (*) - Laumontite
05-0628 (*) - Halite
02-0462 (D) - Illite
Intensity (Counts)
2-Theta Angle, 2θ (°Degrees)

(b)

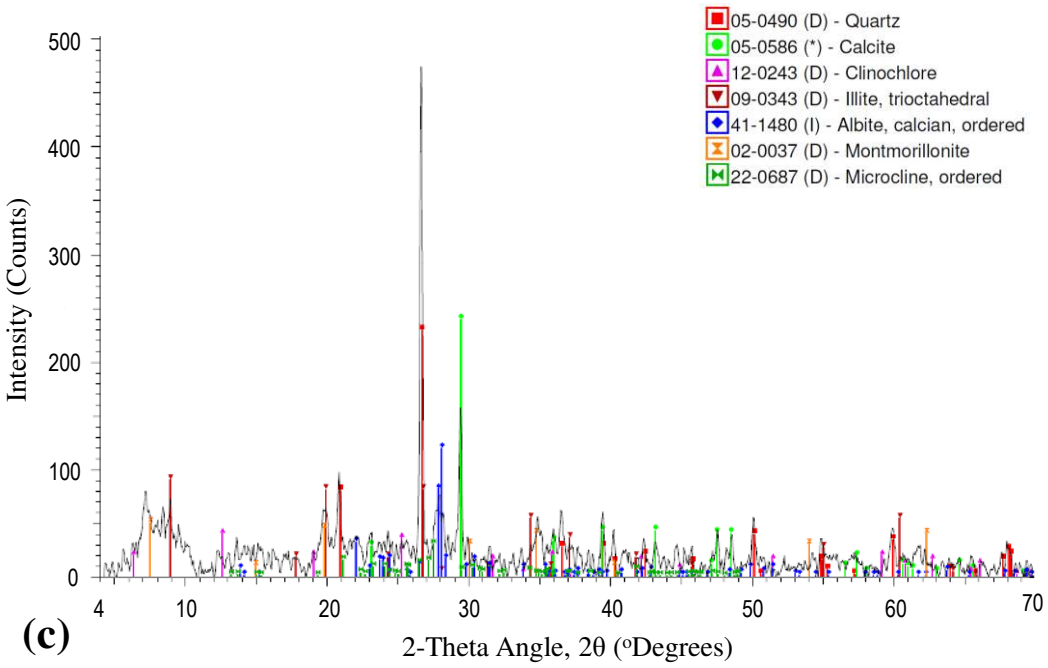

Figure 1. X-ray diffraction (XRD) plots: **(a)** Kaolin; **(b)** Bentonite; and **(c)** Mixture of kaolin and bentonite.

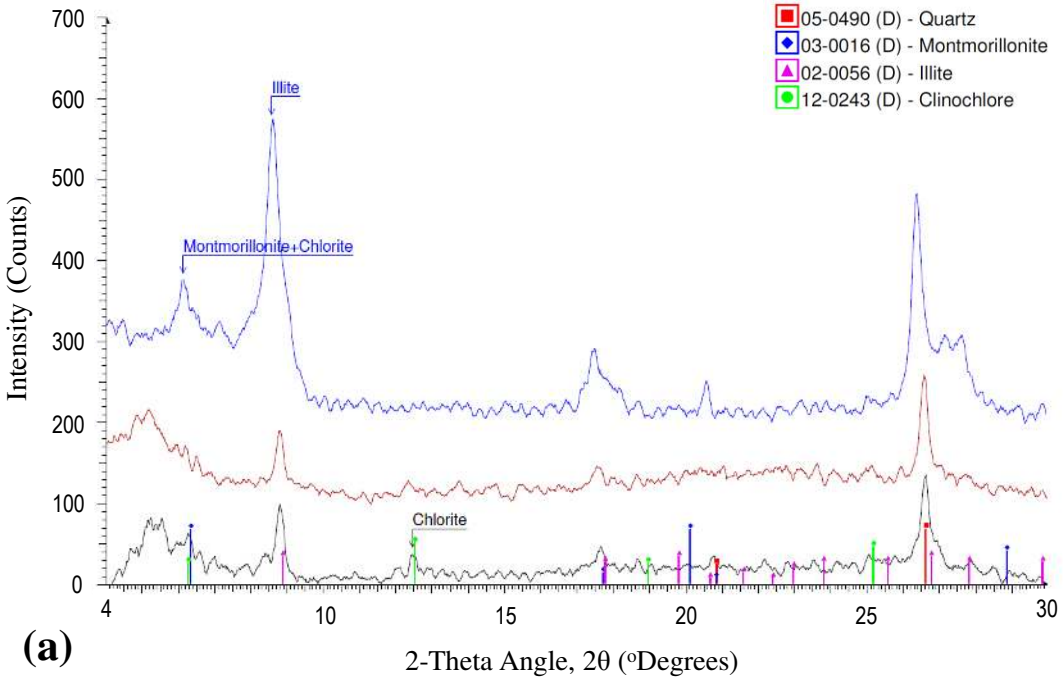
05-0490 (D) - Quartz
03-0016 (D) - Montmorillonite
02-0056 (D) - Illite
12-0243 (D) - Clinochlore
Illite
Montmorillonite+Chlorite
Chlorite
Intensity (Counts)
2-Theta Angle, 2θ (°Degrees)
(a)

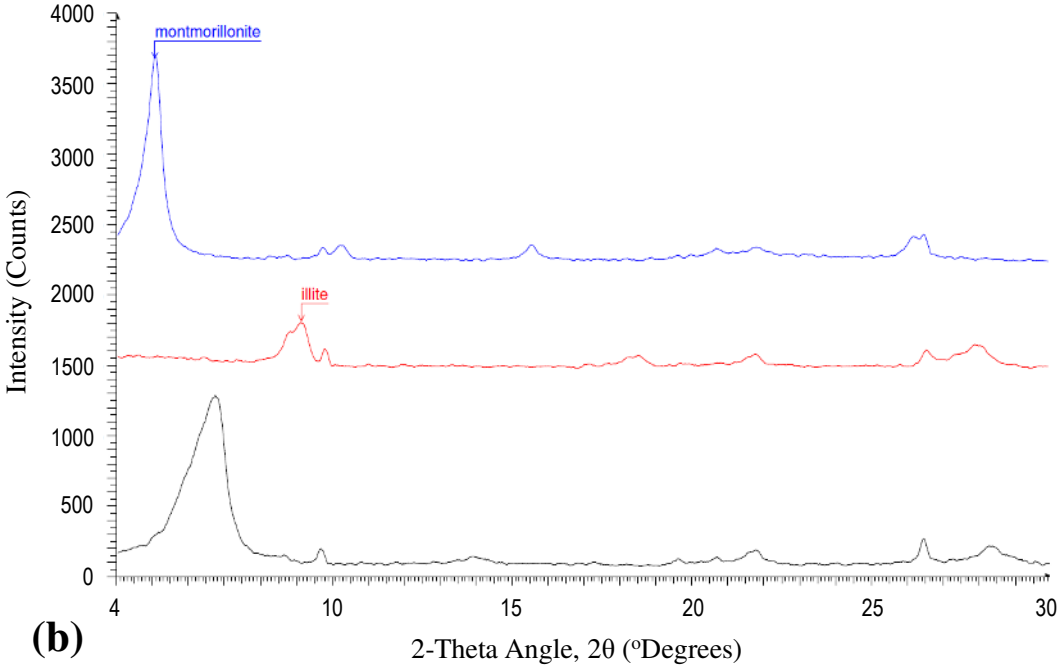
montmorillonite
illite
Intensity (Counts)
2-Theta Angle, 2θ (°Degrees)
(b)

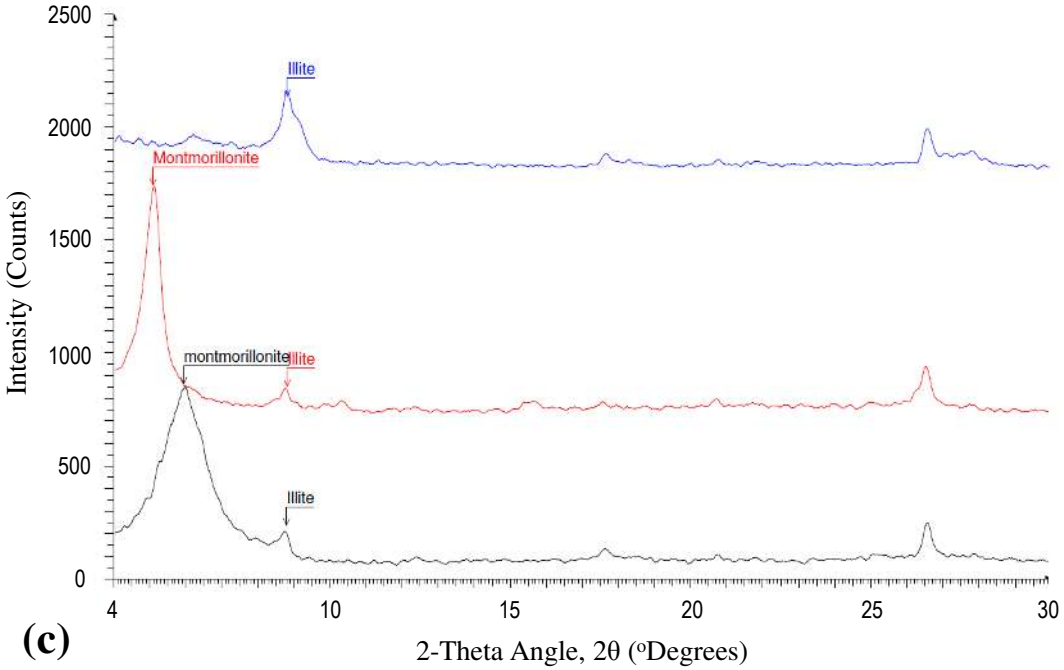

Figure 2. X-ray diffraction (XRD) plots of clay minerals: **(a)** Kaolin; **(b)** Bentonite; and **(c)** Mixture of kaolin and bentonite.

1: Load plate
2: Top porous stone
3: Bottom porous stone
4: Specimen ring
5: Outer ring
6: Vent
7: Loading plunger
8: Wire
9: Temperature controller
10: Power supply
11: Asbestos insulation
12: Coil
13: Drainage valve
14: Strain dial gauge

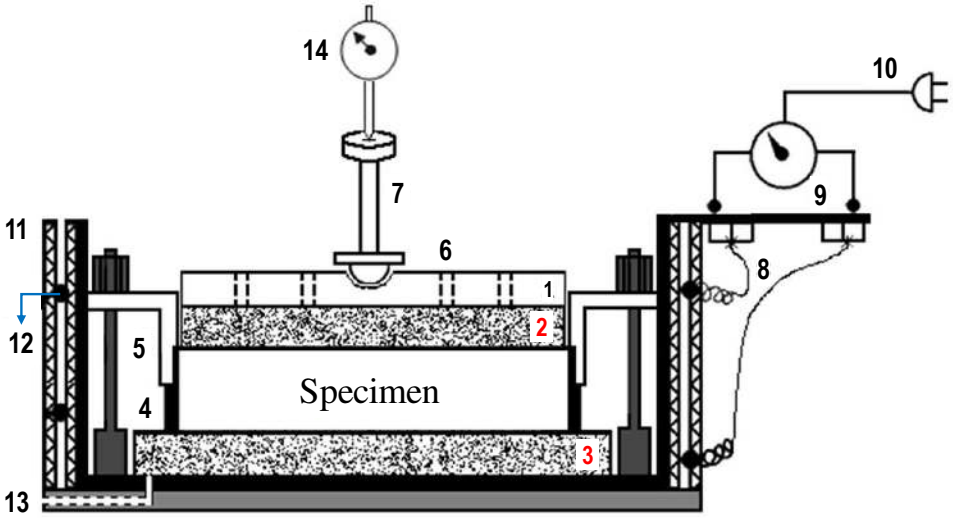

Figure 3. Layout of the apparatus.

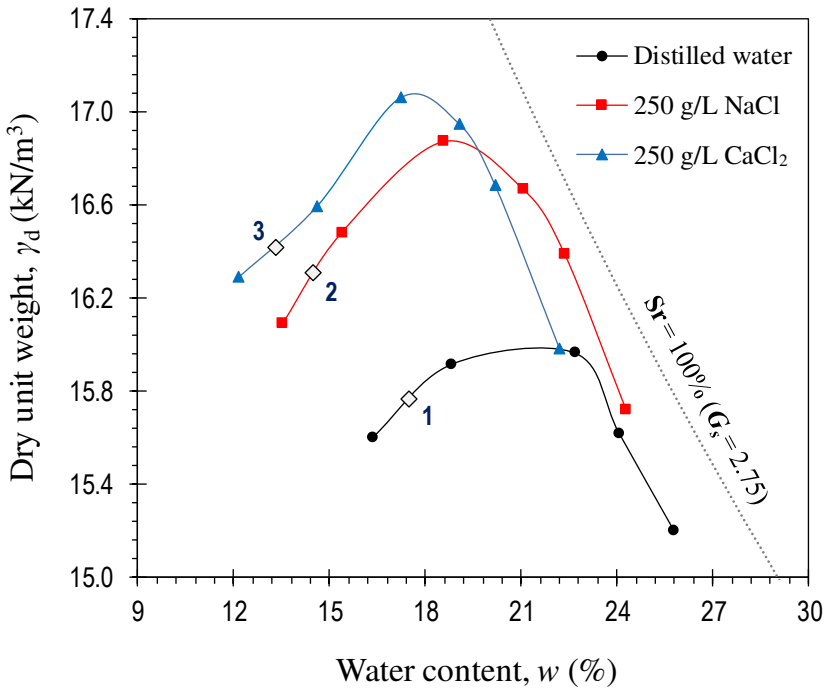

Figure 4. Standard Proctor compaction curves for the samples with different pore water quality (points 1, 2 and 3 show the initial state of the prepared samples).

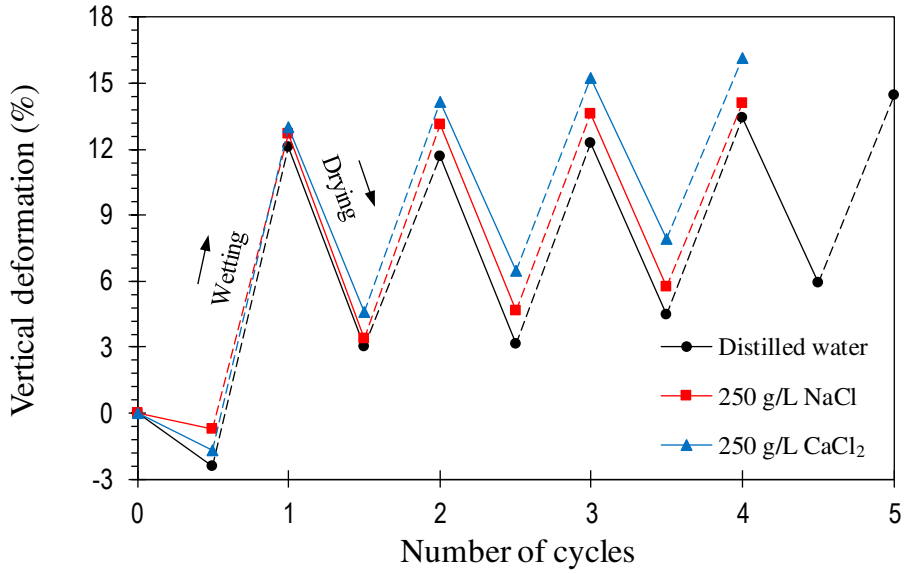

Figure 5. Vertical deformation (in %) during drying and wetting cycles for the samples with different pore water quality.

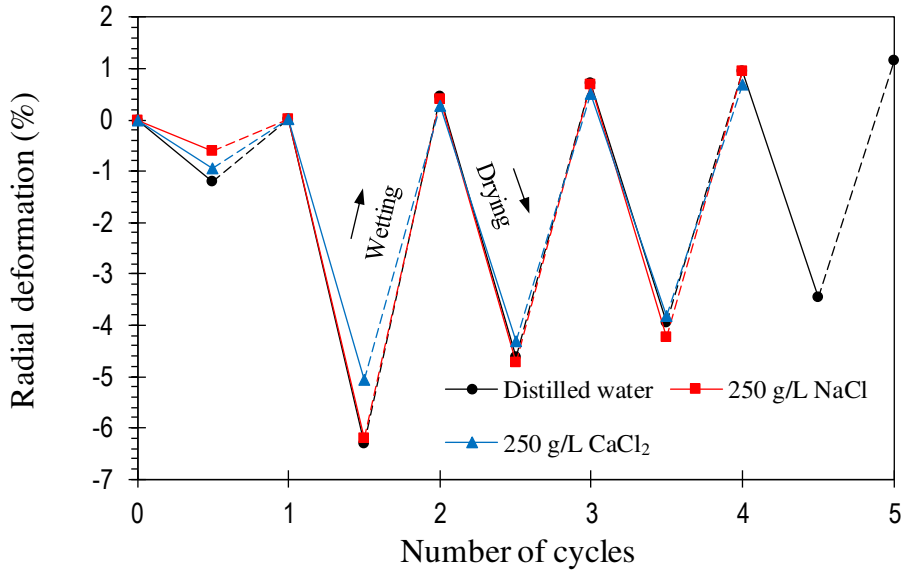

Figure 6. Radial deformation (in %) during drying and wetting cycles for the samples with different pore water quality.

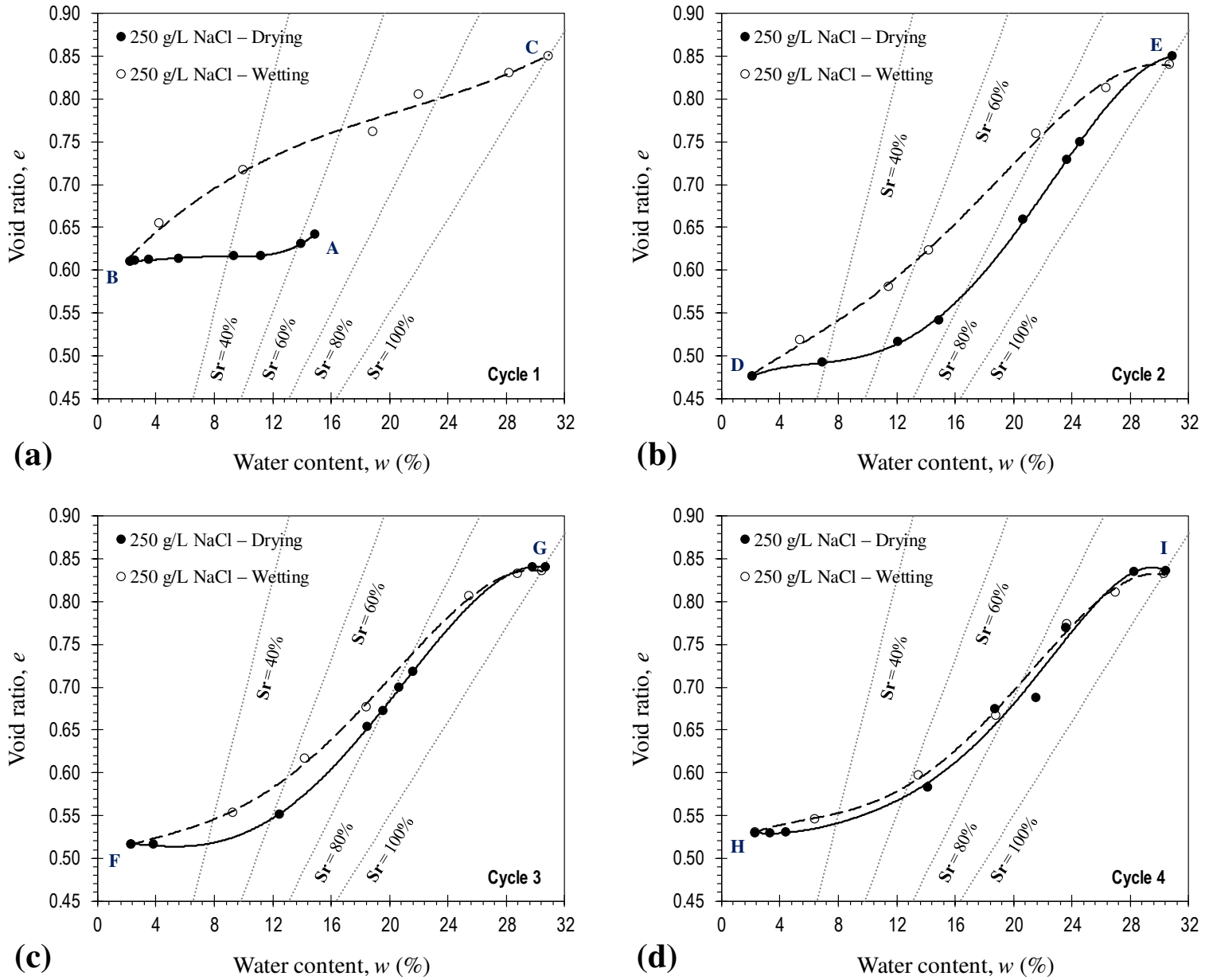

Figure 7. Void ratio–water content shrink–swell paths for the sample with NaCl solution as the pore water: **(a)** Cycle 1; **(b)** Cycle 2; **(c)** Cycle 3; and **(d)** Cycle 4.

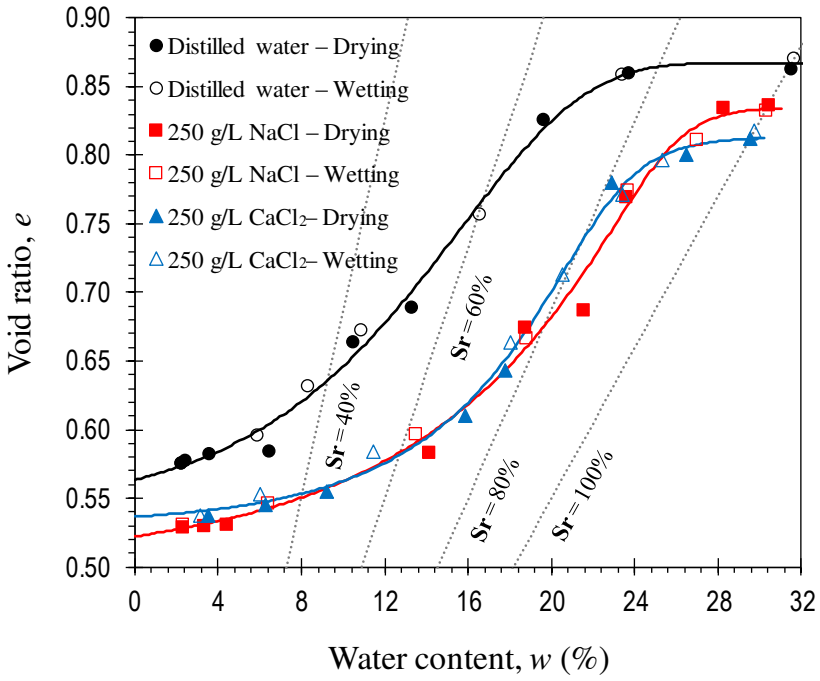

Figure 8. Void ratio–water content shrink–swell paths at equilibrium condition for the samples with different pore water quality.

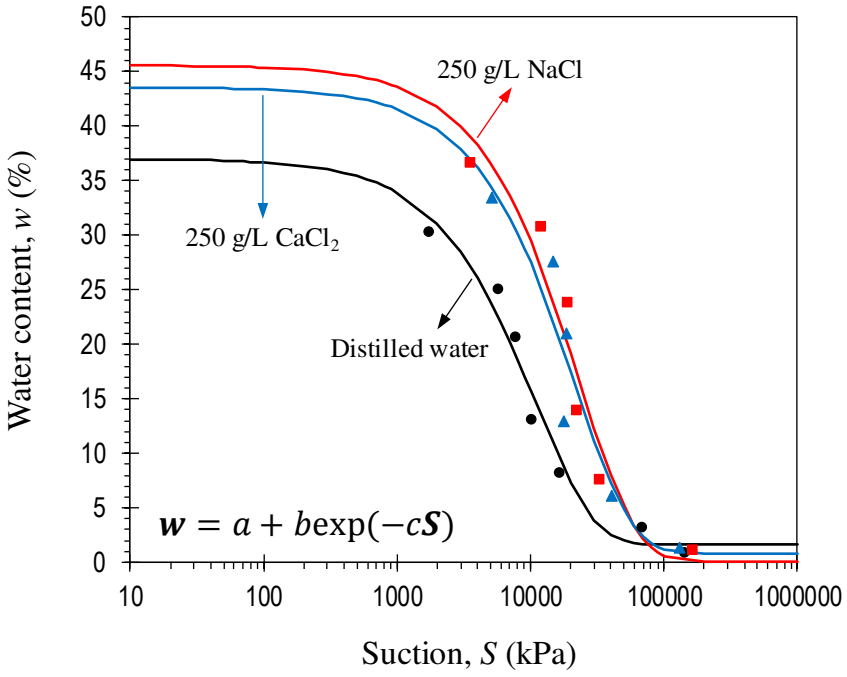

Figure 9. The soil–water characteristic curve (SWCC) for the samples with different pore water quality.

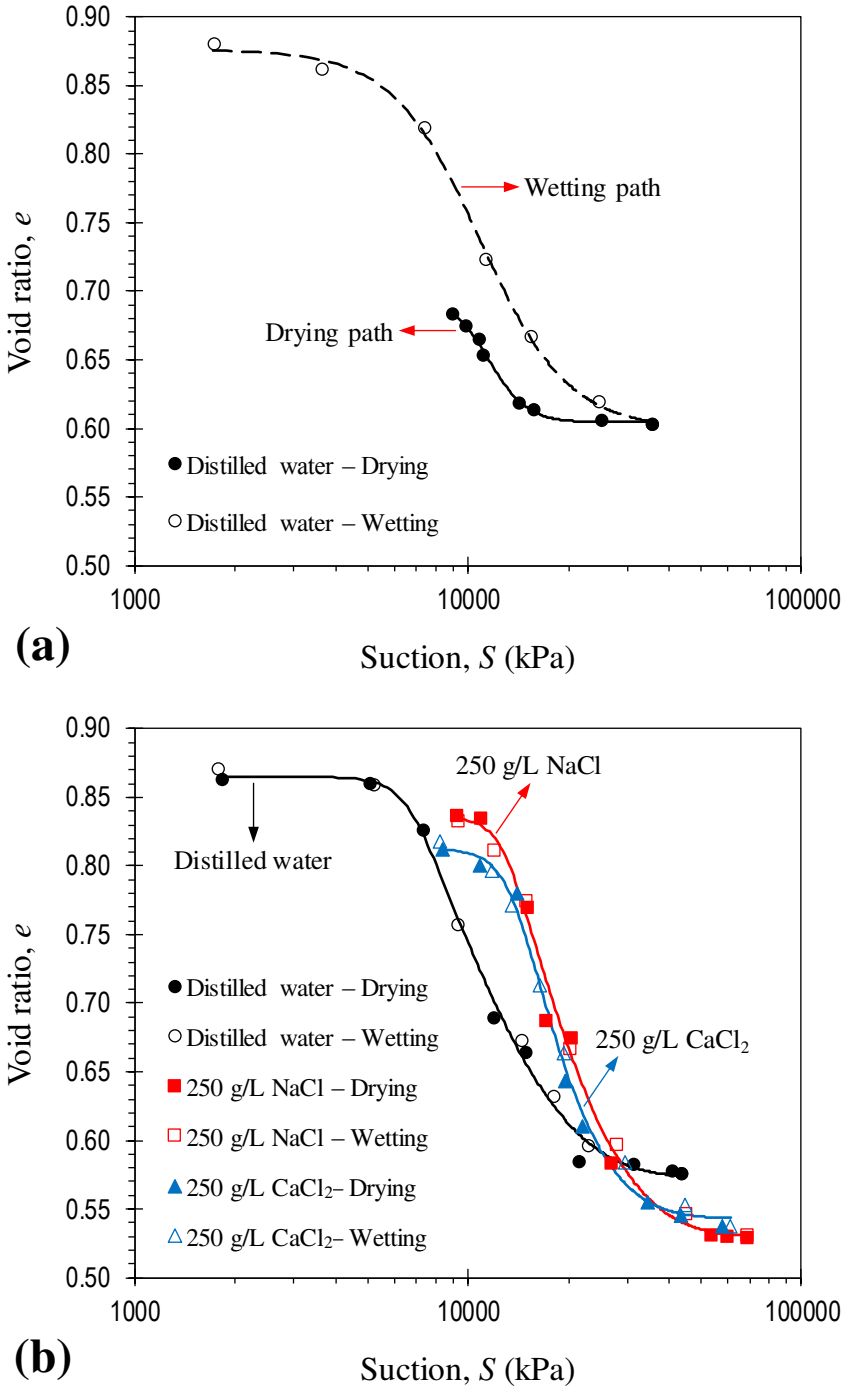

Figure 10. Void ratio–suction shrink–swell paths: **(a)** Cycle 1 for the sample with distilled water as the pore water; and **(b)** Equilibrium condition for the samples with different pore water quality.